Ionospheric Irregularity Influences on GPS Time Delay

Azad A Mansoori[1], Parvaiz A. Khan[1], Shivangi Bhardwaj[2], Roshni Atulkar[2] and P. K. Purohit[2*]

[1]Space Science Laboratory,
Department of Electronics, Barkatullah University,
Bhopal-462026,
India

[2]Department of Applied Sciences,
National Institute of Technical Teachers Training and Research,
Shamla Hills, Bhopal-462002,
India

ABSTRACT

One of most important ionospheric effects on the trans-ionospheric signals is the delay both in range and time. Under this investigation, we have studied the variability of ionospheric range delay in GPS signals. To accomplish this study we have used the GPS measurements at a low latitude station, IISC Bangalore (13.02N, 77.57E) during January 2012 to December 2012. We studied the diurnal, monthly as well as seasonal variability of the range delay. We also selected five intense geomagnetic storms that occurred during 2012 and investigated the variability of delay during these geomagnetic storms. From our study we found the diurnal variability of the range delay is similar to the diurnal pattern observed for TEC. The maximum delay occurs during the month of October while lowest delay is found to occur in the month of December. During summer season the range delay in GPS signals in less while the largest delay occurs during the equinox season. The peak delay and enhancement in delay follows a very good correlation with Dst index.
Key Words: Ionosphere, Range Delay, TEC, Geomagnetic Storm

1. INTRODUCTION

The GPS signals from the satellites while propagating through a disturbed ionospheric medium undergo changes in their characteristics depending on the extent of disturbance. The ionosphere is a dispersive medium, it implies that the ionosphere bends the GPS radio signal from its optical path and it happens due to change in its speed while propagating through various layers of ionosphere. A significant range error is caused by the change in the propagation speed. The ionosphere speeds up the propagation of the carrier phase, whereas it slows down the pseudorange code measurement by an equivalent amount. In other words, the GPS code information is delayed resulting in the pseudorange being measured too long as compared to the geometric distance of the satellite [*Hofmann et al.,* 1992]. So, the receiver-satellite distance will be too short if measured by the carrier phase and is too long if measured by code as compared to the actual distance. The ionospheric time delay is directly proportional to the Total Electron Content (TEC) along the path of propagating signal between the satellite and user (1 meter for 6.15 TEC units on L1 frequency) [*Klobuchar et al.,* 1975]. TEC is highly dependent on many variables such as local time, season, geomagnetic location and the level of solar and magnetic disturbances.
Strong ionospheric disturbances have great impact on performances of the GPS receivers. The ionospheric effects on the GPS receivers have been studied by many researchers [*Doherty et al.,*

2000; *Skone,* 2001; *Bhattacharya et al.,* 2009; *Jain et al.,* 2010]. The positional accuracy of the GPS system is limited by the precision in measuring atmospheric time delay. Precise ionospheric time delay estimation is required for achieving high level of accuracy in determination of position, navigation and geodesy. It is well established that estimation of precise time delay by means of monitoring the clocks on GPS satellites can be limited by the time delay of the earth's ionosphere. At equatorial and low latitudes TEC is highly variable with local time, season and level of solar and magnetic activity. The dominant variability is diurnal due to the large variation in incident solar radiation, so the time delay is also highly variable at low latitudes. At equatorial regions, the earth's magnetic field is horizontal and there is east-west electric field due to the dynamic effect produced by the atmospheric motions. During the day the electric field is eastward and westward during the night. This phenomenon so causes irregularity in the ionospheric condition, hence contribute to the delay mechanism.

The range obtained between the satellite and user by integrating the phase and group refractive indices along the path of GPS signal is different from the true range. The difference between measured range and the true range is known as ionospheric error. This error is negative for the carrier phase pseudoranges and positive for the code pseudoranges [*Komjathy,* 1997]. The delay due to the ionosphere results in range errors which may vary from few meters to tens of meters. The ionosphere is a dispersive medium i.e., its refractive index is a function of the operating frequency [*Kaplan,* 1996; *Mishra and Enge,* 2006). Thus appropriate methods can be adopted for determining the extent of delay due to ionosphere using code observations at L1 (1575.42 MHz) or at both L1 (1575.42 MHz) and L2 (1227.60 MHz) GPS frequencies. Typically ionospheric delays on GPS observations can be reduced by using the combination of two broadcasting frequencies, by using delay model of ionosphere for single frequency users [*Kleusberg,* 1998]. In recent years various ionospheric delay models were proposed [*Klobuchar,* 1986; *Coster et al.,* 1992]. The effects of ionosphere on GPS performances can be considered in two aspects: first during strong ionospheric disturbances and second due to the amplitude and phase variations of GPS signals due to the disturbances, GPS receiver performances are degraded. During these adverse conditions, conventional models can not accurately describe the ionospheric delay. Thus, for achieving precise GPS positioning, the ionospheric effects must be eliminated so that the more precise position could be measured. Hence ionospheric threat models are required to evaluate impact of disturbances on positioning accuracy, which is an important factor for system integrity [*Luo et al.,* 2004].

2. DATA SETS AND METHODOLOGY

To accomplish this study we have made use of three types of data sets; GPS data, Dst index and IMF-Bz. A complete network of GPS receivers has been setup worldwide since last couple of decades, and the observations are carried out regularly. The data obtained in this way is freely available to users. This service commonly known as International GPS Service (IGS) provides the data of hundreds of stations from all parts of the world. GPS navigation and observation data downloaded from the IGS stations is in compressed RINEX format. The time samplings of these data are 30 seconds. The TEC along the path from satellite to receiver, (STEC), at the two GPS frequencies, L1 = f1 = 1.57542 GHz and L2 = f2 = 1.2276 GHz, can be calculated [*Klobuchar,* 1996].

The GPS TEC data used in this study were obtained from the IGS for the IGS station IISC Bangalore (13.02N, 77.57E). However, for the present analysis, the data obtained using code measurement is only used from January to December 2012 for all the days. From the processed data, elevation angle and TEC are used to estimate the time delay values at elevation cut off 40∘.

2.1. ESTIMATION OF IONOSPHERIC DELAY

The most widely used ionospheric model for estimation of ionospheric delay is the grid based ionospheric model. However we have used another model for estimation of ionosheric delay at user position. This method used GPS pseudo-range measurements at both L1 and L2 frequencies. GPS pseudo-range and carrier phase range measurements are estimated based on assumptions that the signal velocity and wavelength are equal to those values valid for an electromagnetic wave propagating in vacuum. However, the ionospheric index of refraction has a non-unit value due to the physical properties of the ionosphere, therefore the assumption that the GPS signal travels at the speed of light in vacuum and with wavelength equal to the wavelength on vacuum is incorrect. The group velocity, however, is less than the speed of light, and caused the group delay. The phase and group velocities can be derived as follows;

$$v_g = \frac{c}{n_g} = \frac{c}{1 + \frac{40.3N}{f^2}} \approx c\left(1 - \frac{40.3N}{f^2}\right)$$

$$v_p = \frac{c}{n_p} = \frac{c}{1 - \frac{40.3N}{f^2}} \approx c\left(1 + \frac{40.3N}{f^2}\right)$$

The phase ionospheric range delay, $\Delta\Phi$, and the group range delay, ΔP, which are caused by the phase advance and the group delay, respectively, can therefore be derived by subtracting the assumed velocity, c, and the true velocities (v_p and v_g) multiplied by the travel time of the signal and can be expressed as follows:

$$\Delta\phi = \int_{path} (n_p - 1)dl = -\frac{40.3}{f^2}\int_{path} Ndl = \frac{40.3}{f^2}TEC$$

$$\Delta P = \int_{path} (n_g - 1)dl = -\frac{40.3}{f^2}\int_{path} Ndl = \frac{40.3}{f^2}TEC$$

The magnitude of the range errors is equal for both carrier phase and pseudo range measurements but with the opposite sign. The quantity $\int_{path} Ndl$ can be evaluated by integrating electron density along the signal path. This quantity represents Total Electron Content (TEC). The Total Electron Content (TEC) is computed and converted into ionospheric delay in meters using a conversion factor. Following relation has been used to get the total ionospheric delay (including receiver bias and P1-P2 bias):

$$TEC = 9.483(R_{L2} - R_{L1}) - TEC_{RC} - TEC_{p1-p2}$$

Where, R_{L1}, is pseudorange at L1 frequency; R_{L2}, is pseudorange at L2 frequency; TEC_{RC}, is receiver bias error/0.351; and TEC_{P1-P2}, is P1-P2 bias error/0.351, respectively.

Therefore, the total ionospheric delay in meters is given as:

$$\Delta I = 0.163 TEC$$

Since the delay due to ionosphere is one of the most important sources of error, in our analysis this delay has been estimated using GPS code observables and methods using TEC values. Ionospheric correction terms from both the methods are applied to the corresponding pseudoranges and user position is estimated.

3.   RESULTS AND DISCUSSIONS

The ionospheric conditions and so the delay changes hour to hour, day to day, season to season as well as during disturbed and quiet solar and geomagnetic conditions. Therefore, we have studied the variability of ionospheric delay diurnally, monthly as well as seasonally.

The interplanetary, solar wind and geomagnetic conditions during the year 2012 are shown in Figure1. The Figure1 shows the variation of Dst index, Kp index, IMF Bz, Solar wind temperature, solar velocity and solar wind density for the year 2012. From the Figure we clearly notice that there has been a mixed type of activity during the year 2012. There were a number of geomagnetic storms some of them intense. Also there was large number of days for which the geomagnetic activity was quite low.
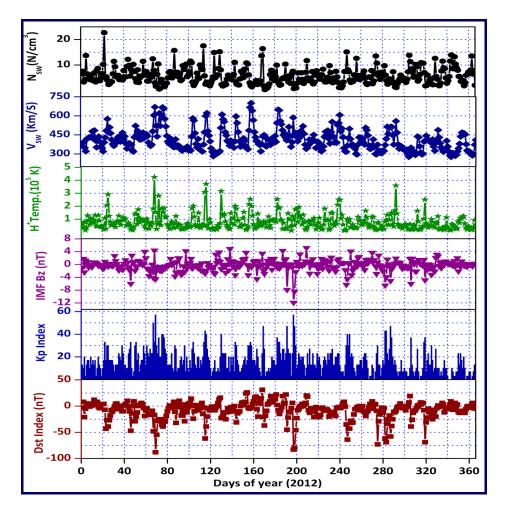

Figure 1: The daily behaviour of various geomagnetic and interplanetary indices during the year 2012

3.1. DIURNAL VARIABILITY

The diurnal variation of ionospheric delay for all the days of each of the twelve months of year 2012 is shown in Figure 2. It can clearly be observed from the figure that the ionospheric delay follows a diurnal pattern similar to that of TEC. It starts increasing in the morning of each day and achieves peak around 0600 to 1200 hrs UT during all months of the year 2012. The delay recorded highest peaks during the months of April, September and October with peak values of about 14 meters while the shallow peaks were observed during the month of June, July, December, January and February with peak values of about 8 meters. The diurnal pattern observed during all the months has same shape with occurrence of diurnal peak around the same times.
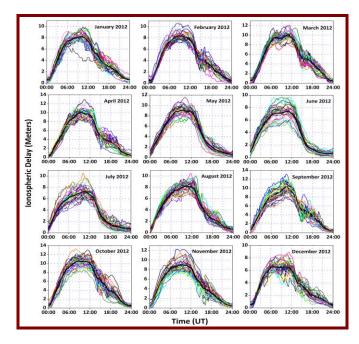
Figure 2: The diurnal variability of the ionospheric delay during all the months of the year 2012.

3.2. MONTHLY VARIABILITY

The month to month variability of the ionospheric range delay for each month of year 2012 is shown in Figure 3. The variability during all the days of each month is averaged to construct the Figure 3. The figure shows that the monthly variation of ionospheric delay is highest during the month of October and reaches a value of 6 meters while the least delay is observed during the month of December with value of 3.6 meters. The ionospheric delay starts increasing from the month of December and achieves peak in the month of March after that it again starts decreasing and reaches minimum in the month June or July. We also notice that the monthly variability follows semi-annual variability.
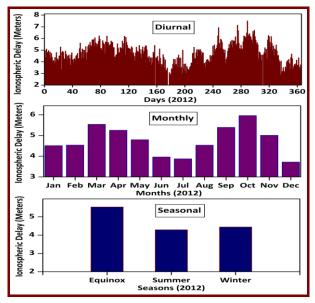

Figure 3: The diurnal, monthly and seasonal variability of the ionospheric delay during the year 2012.

5

3.3. SEASONAL VARIABILITY

We have also studied the seasonal variability of ionospheric delay at IISC Bangalore. The seasonal variability of ionospheric delay during three different seasons of the year 2012 at IISC Bangalore is shown in Figure 3 (bottom panel). The figure shows that the ionospheric delay is maximum during the equinox season with peak value of 5.5 meters while the minimum delay is observed during the summer season with peak value 4.2 meters.

3.4. GEOMAGNETIC VARIATION

We then took the peak values of Dst of all the five storms and the peak enhancement in ionospheric delay during each storm to access the magnitude of correlation between storm intensity index and the ionospheric delay. The scatter plot of peak Dst with enhancement in ionospheric delay during all the five storm events is shown in Figure 4. From the figure we notice the scatter between enhancements produced in the ionospheric delay during each storm with the corresponding intensity of that storm is not much large. We calculated the correlation coefficients of peak ionospheric delay and the enhancement in ionospheric delay with the storm intensity index Dst. We found that both peak values and enhancement in ionospheric delay exhibit a moderate correlation with the storm intensity index, Dst with correlation coefficients 0.60 and 0.65 respectively.
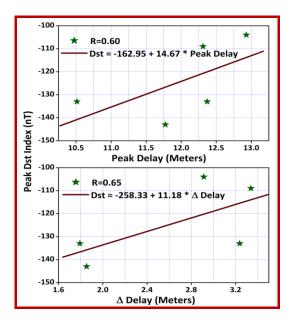

Figure 4: Correlation of storm intensity index, Dst with peak ionospheric delay and enhancement in ionospheric delay.

4. CONCLUSIONS

★ The ionospheric delay follows a typical diurnal pattern achieving a normal diurnal peak around 06:00 to 12:00 UT during all the months of the year**.**
★ The maximum ionospheric delay is observed during the month of October while the minimum delay is observed during the month of December.
★ The maximum delay is observed during equinox season while the minimum delay is observed during the summer season.

- ★ The ionospheric delay is strongly affected during the disturbed geomagnetic conditions. During all the selected five geomagnetic storm events we found a positive enhancement in ionospheric delay.
- ★ A good correlation exists between the peak values of Dst and ionospheric delay as well as between the peak values of Dst and enhancement in ionospheric delay.

ACKNOWLEDGEMENTS

REFERENCES

Bhattacharya, S., Purohit, P. K., & Gwal, A. K. (2009), Ionospheric time delay variation in the equatorial anomaly region during low solar activity using GPS, Ind. J Rad. Spc. Phys., 38, 266-274.

Coster, A. J., Gaposhldn, E. M., & Thornton, L. E. (1992), Real-time ionospheric monitoring system using GPS, J. Inst. Navig., (USA), 39(2), 191-204.

Doherty, P. H., Delay, S., Valladares, C., & Klobuchar, J. (2000), Ionospheric scintillation effects in the equatorial and auroral region, Proceeding of ION-GPS 2000, Salt Lake City, Utah, 662-671.

Hofmann-Wellenhof, B., Lichtenegger, H., & Collins, J. (1992), Global Positioning System: Theory and Practice, 4th edition, Springer-Verlag, Berlin Heidelberg New York.

Jain, A., Tiwari, S., Jain, S., & Gwal, A. K. (2010), TEC response during severe geomagnetic storms near the crest of equatorial ionization anomaly, Ind. J Rad. Spc. Phys., 39, 11-24.

Kaplan, E. D. (1996), Understanding GPS: Principles and Applications, Norwood, MA, Artech House.

Kleusberg, A. (1998), Atmospheric model from GPS, GPS for geodesy, 2nd Edition, Springer, Wien.

Klobuchar, J. A. (1975), Polarization of VHF waves emitted from geostationary satellites, J. Geophys. Res., 80(31), 4387–4389.

Klobuchar, J. A. (1986), Design and Characteristics of the GPS ionospheric time delay algorithm for single frequency users, Proceeding of the PLANS-86 conference, Las Vegas, NY, 280-286.

Klobuchar, J. A. (1996), "Ionospheric Effects on GPS," in Global Positioning System: Theory and Applications, Volume 1, ed. by B. W. Parkinson and J. J. Spilker, American Institute of Aeronautics and Astronautics, Washington, DC.

Komjathy, A. (1997), Global Ionospheric Total Electron Content Mapping Using the Global Positioning System, Ph.D. dissertation, Department of Geodesy and Geomatics Engineering Technical Report No. 188, University of New Brunswick, Fredericton, New Brunswick, Canada, 248pp

Luo, M., Pullen, S., Ene, A., Qiu, D., Waller, T., & Enge, P. (2004), Ionosphere threat to LAAS: Updated model, user impact and mitigations, ION-GNSS 2004, Long Beach, CA, 2771-2785.

Mishra, P., & Enge, P. (2006), Global Positioning System: Signal, Measurements and Performance, 2nd edition, Ganga Jamuna Press, Massachusetts.

Skone, S. H. (2001), The impact of magnetic storm on GPS receiver performance. J. Geodyn, 75(6), 457-472.